High bitrate data transmission in the 8-14 μm atmospheric window using an external Stark-effect modulator with digital equalization

Hamza Dely, Mahdieh Joharifar, Xiaodan Pang, Djamal Gacemi, Toms Salgals, Richard Schatz, Yan-Ting Sun, Thomas Bonazzi, Etienne Rodriguez, Yanko Todorov, et al.

Research Article Vol. 31, No. 5 / 27 Feb 2023 / Optics Express 7259
Optics EXPRESS

High bitrate data transmission in the 8-14 µm atmospheric window using an external Stark-effect modulator with digital equalization

HAMZA DELY,[1,5,*] MAHDIEH JOHARIFAR,[2,5] XIAODAN PANG,[2,3] DJAMAL GACEMI,[1] TOMS SALGALS,[4] RICHARD SCHATZ,[2] YAN-TING SUN,[2] THOMAS BONAZZI,[1] ETIENNE RODRIGUEZ,[1] YANKO TODOROV,[1] ANGELA VASANELLI,[1] ALEKSEJS UDALCOVS,[3] SANDIS SPOLITIS,[4] VJACESLAVS BOBROVS,[4] OSKARS OZOLINS,[2,3,4] SERGEI POPOV,[2] AND CARLO SIRTORI[1]

[1]*Laboratoire de Physique de l'École Normale Supérieure, ENS, CNRS, Université Paris-Cité, Sorbonne Université, F- 75005 Paris, France*
[2]*Department of Applied Physics, KTH Royal Institute of Technology, 106 91 Stockholm, Sweden*
[3]*RISE Research Institutes of Sweden, 164 40 Kista, Sweden*
[4]*Institute of Telecommunications, Riga Technical University, 1048 Riga, Latvia*
[5]*These authors contributed equally to this work*
[*]*hamza.dely@ens.fr*

Abstract: High bitrate mid-infrared links using simple (NRZ) and multi-level (PAM-4) data coding schemes have been realized in the 8 µm to 14 µm atmospheric transparency window. The free space optics system is composed of unipolar quantum optoelectronic devices, namely a continuous wave quantum cascade laser, an external Stark-effect modulator and a quantum cascade detector, all operating at room-temperature. Pre- and post-processing are implemented to get enhanced bitrates, especially for PAM-4 where inter-symbol interference and noise are particularly detrimental to symbol demodulation. By exploiting these equalization procedures, our system, with a full frequency cutoff of 2 GHz, has reached transmission bitrates of 12 Gbit/s NRZ and 11 Gbit/s PAM-4 fulfilling the 6.25 % overhead hard-decision forward error correction threshold, limited only by the low signal-to-noise ratio of our detector.

1. Introduction

At the edge between optics and electronics, mid-infrared (MIR) wavelengths are presently considered for a large number of applications ranging from gas spectroscopy (e.g. pollutant detection) to defense counter measures. Even if carbon dioxide lasers [1] operating at wavelength around 10 µm have been used for many years for research purpose or in factories for material processing, they lack of tunability and cannot be modulated at high frequency. Compact light sources, like laser diodes in the visible and near infrared part of the electromagnetic spectrum, hindered the development of MIR technologies until the 1990's.

The invention of the first semiconductor MIR quantum cascade laser (QCL) in 1994 [2], relying on intraband transitions in semiconductor quantum wells, laid the cornerstone for the conception of a whole new ecosystem of unipolar optoelectronic devices [3] including: quantum well infrared photodetectors (QWIPs) [4], quantum cascade detectors (QCD) [5] and mid-infrared Stark effect-based modulators [6]. The implementation of MIR free-space optical telecommunication links is particularly promising and may be considered as an alternative to 1.5 µm telecom wavelengths [7,8]. In fact, while usual telecom wavelengths radiation can be used

#474209 https://doi.org/10.1364/OE.474209
Journal © 2023 Received 29 Aug 2022; revised 9 Dec 2022; accepted 16 Dec 2022; published 14 Feb 2023

Optics EXPRESS

for ground to space communications, they struggle when it comes to ground to ground free-space applications. MIR wavelengths benefits from two atmospheric transparency windows in this part of the electromagnetic spectrum (4-5 µm and 8-14 µm). Moreover, ~ 10 µm wavelengths are much less sensitive to scattering by all kinds of micro particles suspended in the atmosphere and therefore can propagate over larger distances. Finally, long wavelengths suffer less of the small refractive index fluctuations that make the beam wavefront strongly incoherent, thus very difficult to focus on detectors. Recently, we have demonstrated up to 10 Gbit/s room-temperature MIR free space optics (FSO) system enabled by external modulation with unipolar quantum optoelectronic devices [9]. However, further bitrate improvement was expected with the assist of advanced digital equalization techniques.

In this work, we investigate and demonstrate the performance enhancement that can be brought by usual pre- and post-processing algorithms used in telecommunications in the room-temperature MIR FSO system empowered by unipolar quantum optoelectronic devices, i.e., QCL, Stark-effect modulator and QCD.

2. Free-space optical communication setup

2.1. Optoelectonic devices

Our free-space optical communication system is exclusively made of unipolar quantum optoelectronic devices [9] and is sketched on Fig. 1. A commercial continuous-wave distributed feedback QCL is connected to a DC current source and Peltier-cooled to be operated at room-temperature (20 °C). It emits 80 mW at 8.6 µm wavelength, which is free-space coupled into a quantum Stark effect modulator. The external modulator is a 50µm × 50µm mesa with 8 GHz of 3 dB-bandwidth, designed to operate at 9 µm. It can be tuned by applying a DC voltage bias (energy tuning coefficient around 5 meV V^{-1}). However, a too high offset would reduce the modulation depth as it would impose a lower RF power into the device to avoid field breakdown. Note also that two-thirds of the incident optical power is lost at the facets because of reflections. In this experiment, an arbitrary waveform generator (AWG) of 50 GSa/s is used to generate the modulation signals, which are amplified by a driver amplifier before modulating the incident mid-infrared (MIR) beam at the modulator. The modulator is operating at room temperature.

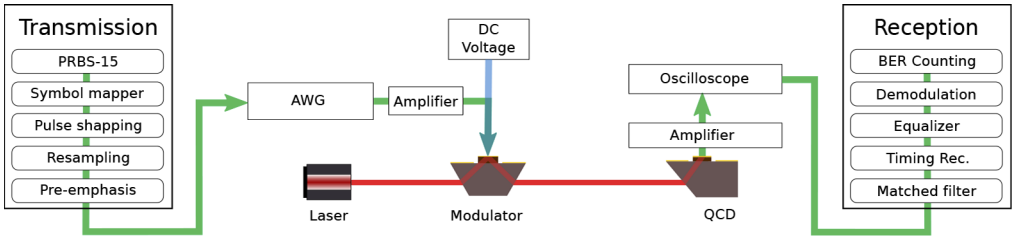

Fig. 1. Schematic of the data transmission setup. A MIR quantum cascade laser emits light to an external modulator connected to a DC voltage drive and an AWG. The modulated beam is collected by a quantum cascade detector. The signal is pre-processed before being sent to the AWG and post-processed before being analyzed with a high-speed oscilloscope.

The output from the modulator is collimated and transmitted over a free-space link of around 70 cm. The MIR receiver at the end of the link is a quantum cascade detector (QCD) operating at room-temperature, placed 1 m away from the laser. It is a 50µm × 50µm mesa QCD with peak responsivity of 6 mA W^{-1} at 8.7 µm. Despite displaying a much lower responsivity than widespread cooled mercury-cadmium-telluride detectors, our device offers a much wider bandwidth (more than 6 GHz instead of 100 MHz to 1 GHz). The incident beam to the QCD is carefully aligned so the output photocurrent is maximized during the measurements. Finally, the

Optics EXPRESS

output signal from the QCD is electrically amplified and captured by a real-time oscilloscope with sampling rate of 40 GSa/s for offline digital signal processing.

2.2. Signal generation and processing

In an attempt to maximize the achievable bitrate, our data traces are both pre- and post-processed digitally at the transmitter and the receiver, respectively [10]. Two modulation formats, namely, binary non-return-to-zero (NRZ) and 4-level pulse amplitude modulation (PAM-4) are employed in this experiment. All the NRZ and the PAM-4 signal traces are generated offline before being sent to the AWG. During the pre-processing at the transmitter, the signal symbols are firstly mapped from repeated pseudo-random bit sequences of $2^{15} - 1$ word length (PRBS-15). Subsequently, the signal levels are adjusted with a new level mapping to tamper any non-linearity the modulator may have. After that the signals are pulse-shaped with a root-raised cosine (RRC) filter to compress its spectral fingerprint. The roll-off the RRC filter is adjusted between 0.1 and 0.5 to optimize the performance for different symbol rates during the measurements. To fit in the AWG memory and to avoid digital artifacts due to sampling, the signal is resampled to match the AWG sampling rate. Finally, a static pre-emphasis filter readjusts the frequency spectrum levels of the signal by normalizing it by the system frequency response to compensate for its irregularities.

On the receiver side, the captured signals at the oscilloscope are converted into digital samples and being post-processed before bit error rate (BER) counting. The traces are firstly convoluted using a matched RRC filter. Then a maximum-variance-based clock recovery is performed to reduce the effects of signal jitter. After that, an adaptive equalization processing based on either a feed-forward equalizer (FFE) or a decision feedback equalizer (DFE) is performed to suppress residual inter-symbol-interference (ISI) and other systematic errors induced through the link. Finally, the recovered signal symbols are demodulated into binary bits for BER performance evaluation.

3. Results

3.1. Frequency response

We first characterize the frequency response of the whole system, including all electronic and optoelectronic devices, in order to configure the RRC pulse-shaper and the pre-emphasis filter. A single tone sweep is performed to scan frequencies up to 9 GHz. The resulting Bode diagram is presented in Fig. 2, with a 3 dB-cutoff frequency of 2 GHz. The frequency response is flat before experiencing a mild decrease (first-order rolloff) with a 10 dB cutoff at 7 GHz. Such a response is a specific characteristic of the intraband devices, while conventional interband telecom devices display relaxation oscillations, generating a resonance before a second order rolloff. As a consequence, for intraband devices the maximum achievable bitrate is enhanced compared to semiconductor laser diodes with the same cutoff frequency.

3.2. BER evaluation

The reliability of our FSO link is evaluated by system transmission measurements. The measured BER after the post-processing are benchmarked against the 6.25 % overhead hard-decision forward error correction (6.25 %-OH HD-FEC) code threshold of 4.5×10^{-3} BER. Compared with some of the high-coding gain soft-decision FEC code types that are normally used for long-haul telecom systems, such a low-coding gain HD-FEC standard is often used for short-reach fiber-optic communications with lower complexity and latency, and has been widely employed in commercial telecom transceivers [11,12], thus considered as a viable benchmark in our studied latency-sensitive MIR FSO cases.

Optics EXPRESS

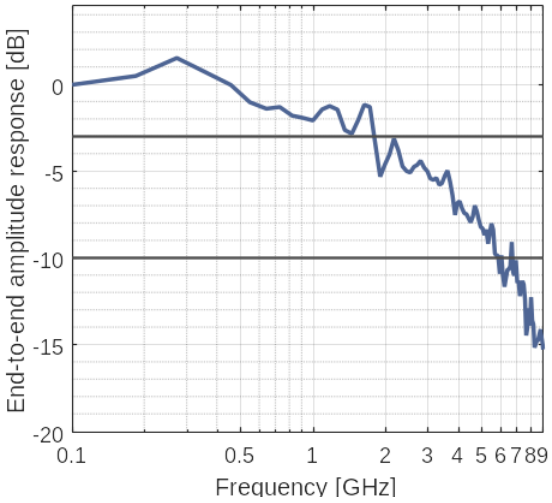

Fig. 2. Bandwidth characterisation of the full system (AWG, modulator, detector, oscilloscope and all other electronic components). The system presents a mild frequency rolloff with a 3 dB bandwidth of 2 GHz and a 10 dB cutoff at 7 GHz.

BER counts for NRZ PRBS patterns as a function of the QCL driving current are presented on Fig. 3 for different equalizer configurations, with bitrates ranging from 10 Gbit/s to 12 Gbit/s. Different FEC thresholds, i.e., 20 %-OH HD-FEC, 6.25 %-OH HD-FEC, and 5.8 %-OH KP4 FEC, are shown with dashed lines for references. As one could expect, the higher the optical power on the detector, the lower is the error count, as an increase of the optical power improves the signal-to-noise ratio (SNR). At maximum power, 11 Gbit/s is achieved without equalization

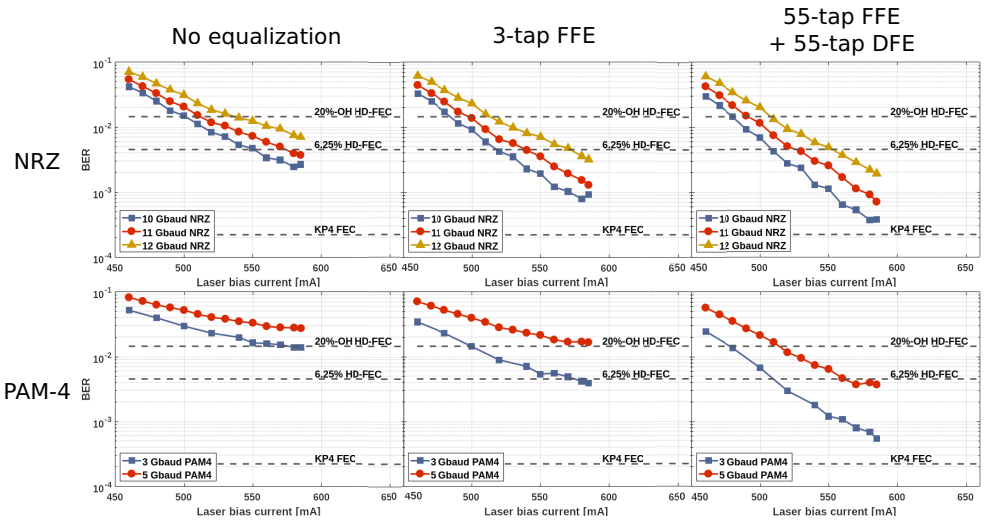

Fig. 3. BER evolution with respect to incident laser power for several equalizer configurations and data bitrates, for both NRZ and PAM-4 with no equalization applied, 3-tap FFE, 55-tap FFE associated to 55-tap DFE. The BER decreases with increasing power due to a better signal to noise ratio. 20 % HD-FEC, 6.25 % HD-FEC and KP4-FEC correction codes thresholds are indicated using dashed lines.

Optics EXPRESS

(Fig. 3 (a)). An equalizer with only 3 feedback taps is enough to correct the systematic errors of the optical link and gets to 12 Gbit/s BER below the 6.25 % HD-FEC limit as shown in Fig. 3 (b). Going to 55-tap does not improve further the result (Fig. 3 (c)). In fact, the strong amplification needed because of the low responsivity of our detector severely impacts the SNR. As our system is noise limited, at fixed optical power, increasing the number of taps of the equalizer does not reduce the BER: from 3 to 55 feedback taps, the BER counts remain almost flat, as it can be seen on Fig. 4, where we summarise the results arising from different combination of pre- and post-processing tap numbers of data traces.

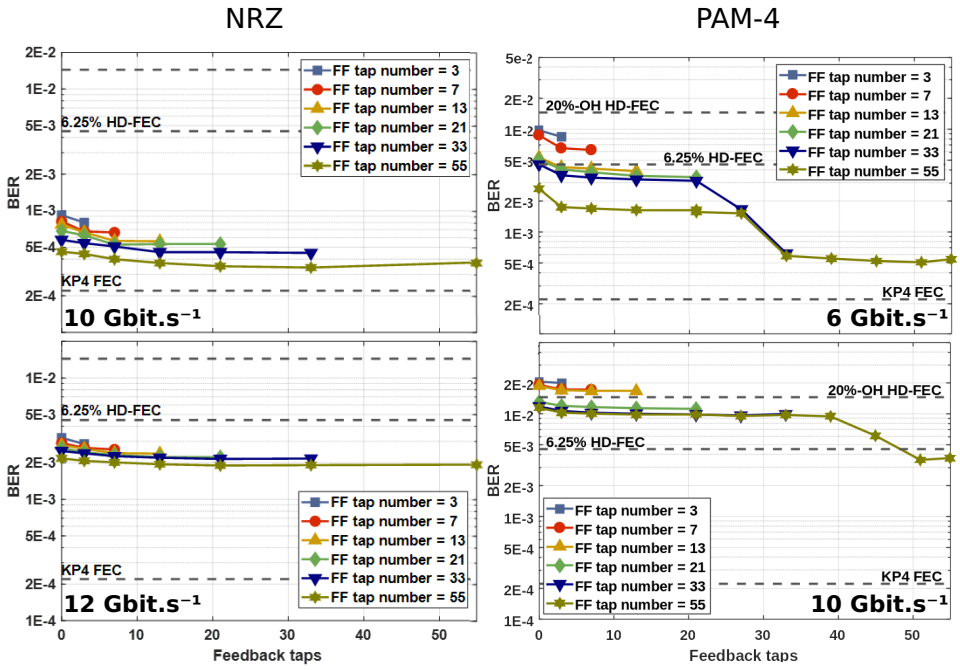

Fig. 4. BER evolution with the number of feedback equalizer tap at maximum optical power for different feed-forward tap numbers. Even though a few taps (feed-back and feed-forward) are enough to equalize our signal, raising their number does not bring any further improvement.

The study is also conducted with PAM-4 PRBS patterns (Fig. 3) with 6 Gbit/s and 10 Gbit/s. As for NRZ, increasing the optical power enhances substantially the BER although these improvements are not as efficient as for NRZ. In fact, the amplitude space for each level shrinks with PAM-4 compared to NRZ but noise is as high as before, therefore extracting symbols is more error-prone. As opposed to NRZ, a large number of FFE and DFE taps is required to recover data frames as illustrated on Fig. 4. Adding FFE taps reduces inter-symbol interferences but adds noise which requires mitigation by increasing the number of DFE taps starting from 20 to 30 taps. The plateau observed at high DFE taps is our signal-to-noise limitation. We achieve 11 Gbit/s PAM-4, with the same noise limitation as for NRZ.

4. Conclusions

We have demonstrated a free-space, high-bitrate mid-infrared link based on unipolar quantum optoelectronic devices and multi-level data coding. 12 Gbit/s NRZ and 10 Gbit/s PAM-4 signals are successfully transmitted over the system and received with BER below the 6.25 %-OH HD-FEC threshold. For the NRZ signals, applying pre- and post-processing does not bring

Optics EXPRESS

substantial improvements as the system is limited by SNR, whereas more significant improvement is observed for the PAM-4 signals after the digital equalization. The heavy electronic noise introduced by the amplifiers due to the low responsivity of our QCD prevents software processing from enhancing the throughput of the link. For the same reason, denser data transmission schemes would not improve this setup even with software processing. Nonetheless, an estimate of a useful link distance can be obtained following Ref. [7]. This model, applied to the results of our setup at 9 µm wavelength, gives over 800 m of transmission range for NRZ signals at 10 Gbit/s with 500 m visibility and 10 cm large optics.

As a perspective, high-performance mid-infrared unipolar detectors embedded in metamaterials, displaying almost 1 A W^{-1} responsivity [13], will be used to improve the detection stage and permit to take full advantage of pre- and post-processing, opening the door to even more complex coding schemes (PAM-8 or higher) and making bitrate in the order of 100 Gbit/s within reach.

Funding. ENS-Thales Chair; Centre National de la Recherche Scientifique (Renatech network); Agence Nationale de la Recherche (ANR-18-CE09-0035 project LIGNEDEMIR); H2020 Future and Emerging Technologies (Project cFLOW, Project Qombs); Région Ile-de-France (DIM SIRTEQ); Vetenskapsrådet (project 2019-05197); European Cooperation in Science and Technology (COST Action CA19111 NEWFOCUS); European Regional Development Fund (No. 1.1.1.2/VIAA/4/20/660 project CARAT); Rīgas Tehniskā Universitāte (Science Support Fund).

Disclosures. The authors declare no conflict of interest.

Data availability. Data underlying the results presented in this paper are not publicly available at this time but may be obtained from the authors upon reasonable request.

References

1. C. K. N. Patel, "Continuous-Wave Laser Action on Vibrational-Rotational Transitions of C O 2," Phys. Rev. **136**(5A), A1187–A1193 (1964).
2. J. Faist, F. Capasso, D. L. Sivco, C. Sirtori, A. L. Hutchinson, and A. Y. Cho, "Quantum cascade laser," Science **264**(5158), 553–556 (1994).
3. J. Teissier, S. Laurent, C. Manquest, C. Sirtori, A. Bousseksou, J. R. Coudevylle, R. Colombelli, G. Beaudoin, and I. Sagnes, "Electrical modulation of the complex refractive index in mid-infrared quantum cascade lasers," Opt. Express **20**(2), 1172–1183 (2012).
4. H. Schneider and H. C. Liu, *Quantum well infrared photodetectors: physics and applications*, no. 126 in Springer series in optical sciences (Springer, Berlin ; New York, 2007).
5. L. Gendron, M. Carras, A. Huynh, V. Ortiz, C. Koeniguer, and V. Berger, "Quantum cascade photodetector," Appl. Phys. Lett. **85**(14), 2824–2826 (2004).
6. E. Dupont, D. Delacourt, V. Berger, N. Vodjdani, and M. Papuchon, "Phase and amplitude modulation based on intersubband transitions in electron transfer double quantum wells," Appl. Phys. Lett. **62**(16), 1907–1909 (1993).
7. C. Sauvage, C. Robert, B. Sorrente, F. Grillot, and D. Erasme, "Study of short and mid-wavelength infrared telecom links performance for different climatic conditions," in *Environmental Effects on Light Propagation and Adaptive Systems II*, K. U. Stein and S. Gladysz, eds. (SPIE, Strasbourg, France, 2019), p. 18.
8. X. Pang, O. Ozolins, S. Jia, L. Zhang, R. Schatz, A. Udalcovs, V. Bobrovs, H. Hu, T. Morioka, Y.-T. Sun, J. Chen, S. Lourdudoss, L. K. Oxenløwe, S. Popov, and X. Yu, "Bridging the Terahertz Gap: Photonics-Assisted Free-Space Communications From the Submillimeter-Wave to the Mid-Infrared," J. Lightwave Technol. **40**(10), 3149–3162 (2022).
9. H. Dely, T. Bonazzi, O. Spitz, E. Rodriguez, D. Gacemi, Y. Todorov, K. Pantzas, G. Beaudoin, I. Sagnes, L. Li, A. G. Davies, E. H. Linfield, F. Grillot, A. Vasanelli, and C. Sirtori, "10 Gbit s^{-1} Free Space Data Transmission at 9 µm Wavelength With Unipolar Quantum Optoelectronics," Laser Photonics Rev. **16**(2), 2100414 (2022).
10. X. Pang, O. Ozolins, R. Lin, L. Zhang, A. Udalcovs, L. Xue, R. Schatz, U. Westergren, S. Xiao, W. Hu, G. Jacobsen, S. Popov, and J. Chen, "200 Gbps/Lane IM/DD Technologies for Short Reach Optical Interconnects," J. Lightwave Technol. **38**(2), 492–503 (2020).
11. "IEEE Standard for Ethernet Amendment 2: Physical Layer Specifications and Management Parameters for 100 Gb/s Operation Over Backplanes and Copper Cables," IEEE Std 802.3bj-2014 (Amendment to IEEE Std 802.3-2012 as amended by IEEE Std 802.3bk-2013) pp. 1–368 (2014).
12. ITU, "OTU4 long-reach interface," ITU-T Recommendation G.709.2/Y.1331.2 (2018).
13. M. Hakl, Q. Lin, S. Lepillet, M. Billet, J.-F. Lampin, S. Pirotta, R. Colombelli, W. Wan, J. C. Cao, H. Li, E. Peytavit, and S. Barbieri, "Ultrafast Quantum-Well Photodetectors Operating at 10 µm with a Flat Frequency Response up to 70 GHz at Room Temperature," ACS Photonics **8**(2), 464–471 (2021).